Experimental sensitivity of future neutrino oscillation experiments

Candidate Number: 133856
Supervisor: Dr. Elisabeth Falk
Word Count: 9283
Date: 18 May 2018

University of Sussex

Abstract

Neutrino oscillation physics has become a major branch of experimental particle physics over the last twenty years, after the observation of flavour oscillations in 1999 and 2001 by the Super-Kamiokande and Sudbury Neutrino Observatory experiments, respectively. Currently, three of the six oscillation parameters are known within a few percent, while the other three are expected to be determined by the current or next generation of experiments. A noteworthy next generation neutrino experiment is the Deep Underground Neutrino Experiment (DUNE), in South Dakota.

In the present dissertation, we review the phenomenology of neutrino oscillations, produce a C++ implementation thereof, and evaluate the sensitivity of the DUNE and Hyper-Kamiokande (Hyper-K) projects to two of the oscillation parameters, namely the mass hierarchy Δm^2_{32} and the CP-violating phase.

We predict that DUNE, with an exposure of 150 kt·MW·year, will reject one of the two mass hierarchies with a significance of at least 5σ even for the least favourable combination of the true parameters. Under either hierarchy, DUNE will reject CP conservation for about 10% of the possible true values of δ_{CP}.

In addition, we predict that Hyper-K, with an exposure of 10 years, has a low sensitivity to the mass hierarchy, with a maximum rejection significance of about 3σ. However we expect its sensitivity to CP violation to be very high, rejecting CP conservation for 75% of all possible values of δ_{CP}, under either hierarchy.

Contents

Preface

This dissertation is a report of the work that was done from September 2017 to April 2018, as part of an MPhys final year project.

Where mathematical derivations are presented that are not a product of our original work, we make it known explicitly and provide a reference to the original author(s).

All graphs shown in this report are results of our neutrino oscillation model, with the exception of figure 3.3 which is a reproduction from the DUNE Conceptual Design Report[1]. The ROOT framework[2] is used to produce the plots. The model is a C++ implementation of the formalism of chapter 2 and the statistics of section 3.1. For reference, it is available publicly at https://github.com/beulard/nuosc. In order to evaluate experimental sensitivities, the code requires predicted integrated event rates to be provided as inputs. In the case of DUNE and Hyper-K, these are estimated from performance estimates of the beamline and detector, and are presented in their respective design reports[1, 3].

Our results are unique but not original, as similar results can be found — and are often referenced throughout the text — in the neutrino oscillation physics literature.

Chapter 1

Introduction

The present dissertation seeks to report about the work that was undertaken to predict the sensitivity of a future neutrino experiment to the underlying oscillation parameters. The production of such results was achieved through the implementation of the quantum mechanical description of neutrino oscillations in a self-contained C++ framework, combined with preliminary models of said experiment.

For this reason, we start the next chapter by introducing the neutrino and the concept of neutrino oscillations with its associated formalism. From the starting point that neutrino flavour eigenstates are different from neutrino mass eigenstates, we derive the probability of a neutrino changing flavour after travelling through empty space.

In our model of a neutrino experiment, we use the assumption that three neutrino flavours exist and that a neutrino produced in a particular flavour will oscillate to the other two and back. Hence we introduce the mixing matrix for three flavours, known as the PMNS matrix, and emphasize the presence in this matrix of an imaginary phase $e^{i\delta_{CP}}$ which for $\delta_{CP} \neq 0$ would generate CP violation in the lepton sector.

Because the neutrino experiments under consideration are long-baseline underground experiments, it is necessary to treat the flavour oscillations not in vacuum but in matter. We show a derivation of the corrections that must be applied in the case where only two neutrinos oscillate and discuss how one can extend this framework to the three neutrino case.

In order to provide motivation for our work, we examine the current state of neutrino oscillations, namely which parameters are known and which parameters require different experiments or more data in order to be determined. We introduce the mass hierarchy problem, which, along with the CP-violating phase δ_{CP}, will be our two oscillation parameters of interest in what follows.

While chapter 2 covers the fundamental principles at work, some elements of statistics also need to be discussed. Evaluating the sensitivity of an experiment requires the formal definition of a relevant test statistic, which then has to be evaluated from our model of the experiment. In order to make the results meaningful, we must also argue about the interpretation of such a test statistic in the context of an experiment which has yet to be performed. The statistics are discussed in the first part of chapter 3.

We then present the oscillation probabilities resulting from our implementation of the formalism of chapter 2 and try to outline some relevant features. The whole purpose of such a model is to apply it to a real neutrino experiment and study the potential outcomes and discoveries that it could bring. We chose the Deep Underground Neutrino Experiment (DUNE) as our main application. Because it is already a very mature project, a multitude of extremely detailed resources are available, such as the four-volume conceptual design report[4] (CDR). Using information and results from the CDR lets us cirumvent the in-depth modelling of a neutrino beam and detector, and focus on the oscillations instead.

This is discussed in detail in the second half of chapter 3.

Finally, we combine all the information of chapter 3 into our predictions of the sensitivity of DUNE to CP violation and to the neutrino mass hierarchy, the two most important unknown oscillation parameters. As a short extra application, we produce similar results for the shorter-baseline Hyper-Kamiokande (Hyper-K) experiment. We examine the differences between DUNE and Hyper-K, and discuss the potential complementarities between the two future experiments.

Chapter 2

Neutrinos and oscillations

We will now give an overview of the theoretical concepts that are used throughout this report. We will present a review of neutrino flavour oscillations in a vacuum, for the commonly considered cases of two and three neutrino flavours. We will derive the oscillation probability for neutrinos in matter with a constant density, in the simpler case of two neutrinos. In the last section, the current state of neutrino oscillations will be reviewed in order to provide context and motivation for the next chapter.

2.1 History of the neutrino

The neutrino particle was first postulated by Wolfgang Pauli in 1930 to explain the continuous energy distribution of the electron in beta decays, in his famous letter to the Physics Institute of Zürich[5].

Its existence was confirmed in 1956 by Cowan and Reines[6] through the observation of anti-neutrinos from a nuclear reactor being captured by protons in a water tank. A number of subsequent experiments were designed to map out the properties of the neutrino and its interactions[7]. As of today, the neutrino is still not fully understood, and neutrino physics has become one of the leading branches of experimental particle physics along with collider physics.

The existence of distinct flavours of neutrinos was first investigated by Bruno Pontecorvo[8] in 1959. He proposed that a weak interaction involving charged leptons (e, μ) discriminates between neutrino flavours, hence a process such as $\nu_\mu + n \to e^- + p$ is forbidden. This was confirmed in 1962 by Danby et al.[9] at the Brookhaven National Laboratory, where they showed that electron-neutrinos and muon-neutrinos were in fact distinct particles. This was also a first hint at the possibility of neutrino flavour oscillations, which Pontecorvo[10] started theorizing in 1967. In 2000, the DONUT experiment[11] reported the observation of tau-neutrino interactions, hence further corroborating the theory of the three neutrino flavours.

As will be discussed later, the fact that a neutrino can change its flavour by propagating through empty space is direct evidence that neutrinos are massive particles, unlike what is initially described by the Standard Model. The 2015 Nobel Prize was awarded to the Super-K and Sudbury Neutrino Observatory (SNO) collaborations for the discovery of neutrino oscillations in 1999 and 2001[1], respectively.

Although neutrino oscillations have been observed, some of the physical parameters that govern this process remain difficult to probe because of the elusiveness of neutrinos: being only involved in weak processes, they require extremely voluminous detectors in order to get the slightest signal. The Deep Underground Neutrino Experiment (DUNE) in

[1] In fact, SNO observed oscillations in matter, known as the MSW effect[12], while Super-K observed oscillations in vacuum.

the United States and the upgrade to Super-Kamiokande, Hyper-Kamiokande in Japan, are examples of future experiments that aim to determine these parameters.

In the Standard Model, there are twelve elementary fermions: six quarks and six leptons (plus their respective antiparticles). The leptons consist of three charged leptons (e, μ, τ) and three corresponding charge-less neutrinos $(\nu_e, \nu_\mu, \nu_\tau)$. The electron neutrino ν_e, for example, is the neutrino which can interact weakly with an electron and a W boson (Fig. 2.1).

Neutrinos, being leptons (colorless) and carrying zero charge, interact only via the weak interaction, which makes them impossible to observe directly. Their existence and their properties can only be inferred from their interactions with other particles. Experimentally, only left-handed neutrinos and right-handed anti-neutrinos are observed. In the Standard Model, this curious property prevents the neutrinos from acquiring a mass through interactions with the Higgs field in the same way that charged leptons do[13]. Hence the Standard Model on its own cannot accurately describe neutrinos, and extensions such as the seesaw mechanism or extra dimensions are needed. This discussion lies beyond the scope of this report since we are only concerned with the phenomenological description of neutrino oscillations, which is achieved via straightforward quantum mechanics in the next section.

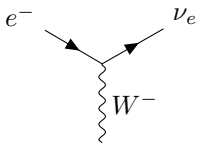

Figure 2.1: The weak vertex for an electron neutrino.

2.2 Neutrino oscillations

We will now introduce the mathematical tools that we use to describe neutrino oscillations.

It is now known experimentally that the neutrino flavours $(\nu_e, \nu_\mu, \nu_\tau)$ mix when propagating through space[14]. This process is structurally similar to the quark generation mixing between down, strange and bottom quarks and is direct evidence that for neutrinos and quarks, the weak eigenstates[2] are not in one-to-one correspondence with the mass eigenstates[3].

In the Standard Model, the W bosons mediate the interactions between up-type and down-type quarks, and between charged leptons and neutrinos. When describing these particles, it is useful to express them either in the weak eigenbasis for interactions or in the mass eigenbasis for free-propagation. For down-type quarks and neutrinos, these bases are not identical: their relationship is conventionally represented by the Cabibbo-Kobayashi-Maskawa (CKM) matrix and the Pontecorvo-Maki-Nakagawa-Sakata (PMNS) matrix, respectively. This allows down-type quarks to interact with up-type quarks of a different generation, or, as we shall see, it allows neutrinos to change their flavour composition as they propagate in empty space.

2.2.1 Neutrino oscillation formalism

The following derivations are heavily inspired by chapter 8 of [7]. Let us consider a general system where there exist n neutrino flavours. We mentioned the two eigenbases of interest: the weak (flavour) eigenstates $|\nu_\alpha\rangle$ where α is a lepton flavour, $\alpha = l_1, l_2, ..., l_n$, and the mass eigenstates $|\nu_i\rangle$, $i = 1, 2, ..., n$. Flavour eigenstates interact with matter through the weak interaction, and hence are the states we observe in Nature. Eigenstates are orthogonal within each basis:

$$\langle \nu_\alpha | \nu_\beta \rangle = \delta_{\alpha\beta}, \quad \langle \nu_i | \nu_j \rangle = \delta_{ij}$$

[2]Weak eigenstate: state which interacts with the W, Z bosons.
[3]Mass eigenstate: state which has definite mass and propagates through space as a wave.

and the two bases are related by a $n \times n$ unitary matrix U:

$$|\nu_\alpha\rangle = \sum_i U_{\alpha i} |\nu_i\rangle \tag{2.1}$$

$$|\nu_i\rangle = \sum_\gamma (U^\dagger)_{i\gamma} |\nu_\gamma\rangle = \sum_\gamma U^*_{\gamma i} |\nu_\gamma\rangle \tag{2.2}$$

$$U^\dagger U = 1,$$

where greek letters denote indices in the flavour basis and latin letters denote indices in the mass basis.

The mass eigenstates are solutions of the free Hamiltonian in a vacuum, hence they are stationary states and evolve in time as $|\nu_i(x,t)\rangle = \mathrm{e}^{-\mathrm{i}E_i t} |\nu_i(x,0)\rangle$, where $|\nu_i(x,0)\rangle = \mathrm{e}^{\mathrm{i}px} |\nu_i\rangle$ for a plane wave neutrino produced at $x = 0$. Hence a neutrino produced as a flavour eigenstate α would have the following time dependence:

$$\begin{aligned}
|\nu_\alpha(x,t)\rangle &= \sum_i U_{\alpha i} |\nu_i(x,t)\rangle \\
&= \sum_i U_{\alpha i} \mathrm{e}^{-\mathrm{i}E_i t} \mathrm{e}^{\mathrm{i}px} |\nu_i\rangle \\
&= \sum_{i,\gamma} U_{\alpha i} U^*_{\gamma i} \mathrm{e}^{\mathrm{i}px} \mathrm{e}^{-\mathrm{i}E_i t} |\nu_\gamma\rangle \quad \text{(using eq. 2.2)}.
\end{aligned}$$

Note that we are working in natural units where $c = \hbar = 1$ for clarity. When implementing this formalism in code, the units must be restored using the usual conversion factors in order to get accurate numerical results. The transition amplitude to a flavour β is thus

$$A_{\alpha\to\beta}(x,t) = \langle \nu_\beta | \nu_\alpha(x,t) \rangle = \sum_i U^*_{\beta i} U_{\alpha i} \mathrm{e}^{\mathrm{i}px} \mathrm{e}^{-\mathrm{i}E_i t} \quad \text{(using eq. 2.1)}.$$

By assuming that all neutrinos have small masses, and thus are highly relativistic, we are able to perform a binomial approximation on their energy:

$$E_i = \sqrt{m_i^2 + p^2} \simeq p + \frac{m_i^2}{2p} \simeq E + \frac{m_i^2}{2E}, \tag{2.3}$$

where we call $E \approx p$ the neutrino energy at the source[4]. We call L the distance from the neutrino source to the detector, known as the baseline. Under our relativistic assumption, we have $L \approx t$. Going back to the transition amplitude,

$$\begin{aligned}
A_{\alpha\to\beta}(L,E) &= \sum_i U^*_{\beta i} U_{\alpha i} \exp\left(\mathrm{i}EL - \mathrm{i}(E + \frac{m_i^2}{2E})L\right) \\
&= \sum_i U^*_{\beta i} U_{\alpha i} \exp\left(-\mathrm{i}\frac{m_i^2 L}{2E}\right),
\end{aligned}$$

The transition probability is then

$$\begin{aligned}
P_{\alpha\to\beta}(L,E) &= |A_{\alpha\to\beta}(L,E)|^2 \\
&= \sum_i \sum_j U_{\alpha i} U^*_{\beta i} U^*_{\alpha j} U_{\beta j} \exp\left(-\mathrm{i}\frac{\Delta m^2_{ij}}{2}\frac{L}{E}\right),
\end{aligned} \tag{2.4}$$

[4] As pointed out by Cohen, Glashow and Ligeti[15], we are taking a shortcut here by assuming that the weak eigenstate comes out as a linear superposition of mass eigenstates with equal energies. However our description leads to identical oscillation formulae as a more physically rigorous one where particle entanglement after the interaction is taken into account. We choose to keep this derivation and skip the details for the sake of simplicity.

where $\Delta m^2_{ij} = m^2_i - m^2_j$ is the mass-squared difference between two mass eigenstates. The analysis is similar when considering anti-neutrinos except that U must be replaced by U^* everywhere and vice-versa.

The formula we have derived here is the general probability of oscillation from a flavour eigenstate $|\nu_\alpha\rangle$ to another flavour eigenstate $|\nu_\beta\rangle$. This effectively describes the probability that after travelling a distance L, the neutrino wavefunction will collapse into a β flavoured neutrino if it interacts in our detector. In the following sections, we apply this formalism to two-neutrino and three-neutrino systems.

2.2.2 Two-neutrino oscillations

The case for two neutrino eigenstates is the simplest to consider. The unitary nature of the mixing matrix U and the arbitrarity of the complex phases of quantum states reduces the number of observable mixing parameters to one[16]. An enlightening way to write the mixing matrix is[7]

$$\begin{bmatrix}\nu_\mu \\ \nu_\tau\end{bmatrix} = \begin{bmatrix}\cos\theta & \sin\theta \\ -\sin\theta & \cos\theta\end{bmatrix}\begin{bmatrix}\nu_1 \\ \nu_2\end{bmatrix}, \tag{2.5}$$

where θ is called the mixing angle. We see here that the two eigenbases are analogous to two sets of Cartesian axes in two dimensions, one being rotated by an angle θ with respect to the other.

We use the μ and τ flavours here in reference to the atmospheric neutrino experiment at Super-Kamiokande[14] (Super-K): for neutrinos produced by cosmic rays in the atmosphere, it is a good approximation to consider a two-neutrino oscillation between the μ and τ flavours, and to neglect the $\nu_\mu \to \nu_e$ channel. This simple mixing matrix can be substituted in eq. 2.4 to obtain a more concrete oscillation probability:

$$\begin{aligned} P_{\nu_\mu\to\nu_\tau}(L,E) &= U^2_{\mu1}U^2_{\tau1} + U^2_{\mu2}U^2_{\tau2} \\ &\quad + U_{\mu1}U_{\tau1}U_{\mu2}U_{\tau2}\left[\exp\left(-\mathrm{i}\frac{\Delta m^2_{12}L}{2E}\right) + \exp\left(-\mathrm{i}\frac{\Delta m^2_{21}L}{2E}\right)\right] \\ &= \cos^2\theta\sin^2\theta\ \left[2 - 2\cos\frac{\Delta m^2_{21}L}{2E}\right] \\ &= \sin^2(2\theta)\sin^2\left(\frac{\Delta m^2}{4}\frac{L}{E}\right), \end{aligned} \tag{2.6}$$

where in the first step we have used the fact that $\Delta m^2_{12} = m^2_1 - m^2_2 = -(m^2_2 - m^2_1) = -\Delta m^2_{21}$ to bring the exponentials into cosine form. Note that there are only two mass eigenstates here, hence we define $\Delta m^2 \equiv \Delta m^2_{21}$.

This example is particularly informative, as one can clearly see the role of each parameter in the oscillation probability. The first term is a constant which depends on the mixing angle, and must be determined by experiment. For $\theta = \frac{\pi}{4}$, the mixing is maximal and the probability is allowed to increase up to 100%. The second term is manifestly oscillatory. Its frequency is determined by the mass difference Δm^2, which may also be determined by fitting experimental data. Note also that if the mass squared difference is zero, the oscillation probability is zero. This implies that oscillations are only possible if at least one of the mass eigenstates has a non-zero mass. Evidently, since there are only two flavours, the probability of ν_μ "survival" is

$$P_{\nu_\mu\to\nu_\mu}(L,E) = 1 - P_{\nu_\mu\to\nu_\tau}(L,E).$$

2.2.3 Three neutrino oscillations

When we consider three eigenstates, the number of parameters is increased to four[16]: three mixing angles θ_{12}, θ_{13} and θ_{23}, and an imaginary phase $\mathrm{e}^{\mathrm{i}\delta_{CP}}$. This so called CP-

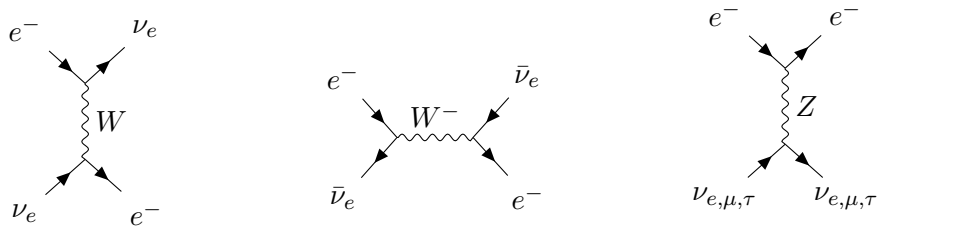

(a) Electron-neutrino scattering.

(b) Anti-ν_e scattering.

(c) Scattering through Z boson affects all flavours equally.

Figure 2.2: The three possible tree-level interactions of neutrinos with atomic electrons in matter.

violating phase gives rise to a difference between oscillation probabilities of neutrinos and anti-neutrinos, hence it allows violation of the charge-parity (CP) symmetry. The mixing matrix can be written in a suggestive way as

$$U_{\text{PMNS}} = \begin{bmatrix} 1 & 0 & 0 \\ 0 & c_{23} & s_{23} \\ 0 & -s_{23} & c_{23} \end{bmatrix} \begin{bmatrix} c_{13} & 0 & s_{13}\mathrm{e}^{-\mathrm{i}\delta_{CP}} \\ 0 & 1 & 0 \\ -s_{13}\mathrm{e}^{\mathrm{i}\delta_{CP}} & 0 & c_{13} \end{bmatrix} \begin{bmatrix} c_{12} & s_{12} & 0 \\ -s_{12} & c_{12} & 0 \\ 0 & 0 & 1 \end{bmatrix}, \tag{2.7}$$

where $c_{ij} = \cos(\theta_{ij})$ and $s_{ij} = \sin(\theta_{ij})$. This form is analogous to a 3D rotation around three Euler angles, except for the appearance of δ_{CP} in the "13" rotation.

Unlike in the two-neutrino case, substituting this mixing matrix into eq. 2.4 turns out not to be very insightful. It is important however to underline all the oscillation parameters that are present here. Along with the four mixing parameters in the PMNS matrix, we have three mass squared differences Δm^2_{31}, Δm^2_{32} and Δm^2_{21}, of which two are independent since $\Delta m^2_{32} + \Delta m^2_{21} = \Delta m^2_{31}$. This leaves six independent parameters that must be determined by oscillation experiments. In section 2.2.5, we will go over the current state of our knowledge of these parameters, which will provide motivation for the work presented in chapter 3.

2.2.4 Neutrino oscillations in matter

So far we have only discussed neutrino oscillations in vacuum, where no weak interactions take place. In matter, where atoms are present, neutrinos can undergo coherent forward scattering off of atomic electrons, modifying the oscillation probability over large enough distances. This is known as the Mikheyev-Smirnov-Wolfenstein (MSW) effect[17, 18], or simply matter effect.

A neutrino can scatter either by exchanging a $W^\pm$ boson — known as charged current (CC) interaction — or by exchanging a Z boson — neutral current (NC) interaction. The neutral current interaction is experienced equally by all three flavours (fig. 2.2c), hence it does not have an effect on the relative propagation phases, and causes no change in the oscillation probability. The charged current is specific to the neutrino flavour. Since only electrons are present in matter, only electron neutrinos are subject to CC interactions (figs. 2.2a, 2.2b). Hence electron neutrinos propagating in matter pick up a different phase than if they were propagating in empty space. This can be implemented in the oscillation formalism by adding a potential term to the Hamiltonian for electron neutrinos only. This term will be proportional to the density of matter and to the weak coupling constant[7].

In what follows, we derive the corrections that must be applied to the oscillation formalism for two neutrino flavours, in order to accurately describe oscillations in matter. This derivation is inspired by section 8.9 of Kai Zuber's textbook[7] and Stefania Ricciardi's notes on oscillations in matter[19].

We start from the time evolution of two mass eigenstates (Schrödinger's equation):

$$\begin{aligned}
\mathrm{i}\frac{\mathrm{d}}{\mathrm{d}t}\begin{bmatrix}\nu_1\\ \nu_2\end{bmatrix} &= \hat{H}_{\text{mass}}\begin{bmatrix}\nu_1\\ \nu_2\end{bmatrix}\\
&= \begin{bmatrix}E_1 & 0\\ 0 & E_2\end{bmatrix}\begin{bmatrix}\nu_1\\ \nu_2\end{bmatrix}\\
&= \frac{1}{2E}\begin{bmatrix}m_1^2 & 0\\ 0 & m_2^2\end{bmatrix}\begin{bmatrix}\nu_1\\ \nu_2\end{bmatrix} + \begin{bmatrix}E & 0\\ 0 & E\end{bmatrix}\begin{bmatrix}\nu_1\\ \nu_2\end{bmatrix},
\end{aligned} \tag{2.8}$$

where in the last step we used the approximation of eq. 2.3. The second term is a multiple of the identity, and only contributes a common phase to the wavefunctions ν_1 and ν_2. It does not affect the oscillations, and will be discarded in what follows. Now we transform into the flavour basis by using $|\nu_{\text{mass}}\rangle = U^\dagger |\nu_{\text{flavour}}\rangle$ (eq. 2.2), and multiply by U on the left:

$$\begin{aligned}
&\mathrm{i}\frac{\mathrm{d}}{\mathrm{d}t}\left(U^\dagger\begin{bmatrix}\nu_e\\ \nu_\mu\end{bmatrix}\right) = \frac{1}{2E}\begin{bmatrix}m_1^2 & 0\\ 0 & m_2^2\end{bmatrix}U^\dagger\begin{bmatrix}\nu_e\\ \nu_\mu\end{bmatrix}\\
\Longrightarrow\ &\mathrm{i}\underbrace{UU^\dagger}_{=1}\frac{\mathrm{d}}{\mathrm{d}t}\begin{bmatrix}\nu_e\\ \nu_\mu\end{bmatrix} = \underbrace{\frac{1}{2E}U\begin{bmatrix}m_1^2 & 0\\ 0 & m_2^2\end{bmatrix}U^\dagger}_{\equiv\hat{H}_{\text{flavour}}}\begin{bmatrix}\nu_e\\ \nu_\mu\end{bmatrix}.
\end{aligned}$$

For this illustration, our two flavours are ν_e and ν_μ because matter effects play an important role in the oscillations between those two, for example in long baseline experiments, or for solar neutrinos. We use the explicit form of U for two neutrinos (eq. 2.5) to determine $\hat{H}_{\text{flavour}}$. The result is

$$\hat{H}_{\text{flavour}} = \frac{\Delta m^2}{4E}\begin{bmatrix}-\cos 2\theta & \sin 2\theta\\ \sin 2\theta & \cos 2\theta\end{bmatrix}, \tag{2.9}$$

where $\Delta m^2 = m_2^2 - m_1^2$, and we have subtracted a multiple of the identity. Our goal, after introducing the extra potential in matter, will be to express the flavour Hamiltonian in this form, albeit with different Δm^2 and θ, and to relate it to the mass eigenstates in matter. This will ensure that we can simply apply the steps of section 2.2.2 and directly obtain the oscillation formula.

In matter, the electron neutrinos interact with electrons, so we must add a potential term V_e to the Hamiltonian. For simplicity, we assume that this term is constant, i.e. that the density of matter is constant. This assumption is fairly accurate for neutrinos propagating in the Earth's crust, but not for solar neutrinos, for example. The Hamiltonian in matter is

$$\hat{H}^m_{\text{flavour}} = \frac{\Delta m^2}{4E}\begin{bmatrix}-\cos 2\theta & \sin 2\theta\\ \sin 2\theta & \cos 2\theta\end{bmatrix} + \begin{bmatrix}V_e & 0\\ 0 & 0\end{bmatrix}. \tag{2.10}$$

Again, we subtract a multiple of the identity $V_e/2$ without affecting the oscillations:

$$\hat{H}^m_{\text{flavour}} = \frac{\Delta m^2}{4E}\begin{bmatrix}-\cos 2\theta + A & \sin 2\theta\\ \sin 2\theta & \cos 2\theta - A\end{bmatrix}, \tag{2.11}$$

where $A = 2EV_e/\Delta m^2$. This form of the Hamiltonian implies that the mass eigenstates in the vacuum are not mass eigenstates in matter. Indeed, if we go back to the mass eigenbasis, we see that the Hamiltonian is no longer diagonal:

$$\begin{aligned}
\hat{H}^m_{\text{mass}} &= U^\dagger \hat{H}^m_{\text{flavour}} U\\
&= \frac{\Delta m^2}{4E}\begin{bmatrix}A\cos 2\theta - 1 & A\sin 2\theta\\ A\sin 2\theta & 1 - A\cos 2\theta\end{bmatrix}.
\end{aligned}$$

It can be diagonalized by transforming the mass eigenvector such that

$$\mathrm{i}\frac{\mathrm{d}}{\mathrm{d}t}\begin{bmatrix}\nu_{1m}\\ \nu_{2m}\end{bmatrix} = \underbrace{\frac{1}{2E}\begin{bmatrix}m_{1m}^2 & 0\\ 0 & m_{2m}^2\end{bmatrix}}_{\equiv \hat{H}^m_{\text{mass, diag}}}\begin{bmatrix}\nu_{1m}\\ \nu_{2m}\end{bmatrix}, \tag{2.12}$$

where ν_{1m} and ν_{2m} are the mass eigenstates in this new basis, and the eigenvalues m_{1m}^2 and m_{2m}^2 obey

$$\Delta m_m^2 = m_{2m}^2 - m_{1m}^2 = \Delta m^2\sqrt{(\cos 2\theta - A)^2 + \sin^2 2\theta}. \tag{2.13}$$

Equation 2.12 is the equivalent of eq. 2.8 in matter. The matter interaction has the effect of changing the mass difference between our mass eigenstates. This will effectively change the frequency of the oscillations. We now try to relate the new mass eigenstates to the old flavour eigenstates. We can always define

$$\begin{bmatrix}\nu_e\\ \nu_\mu\end{bmatrix} \equiv \underbrace{\begin{bmatrix}\cos\theta_m & \sin\theta_m\\ -\sin\theta_m & \cos\theta_m\end{bmatrix}}_{U_m}\begin{bmatrix}\nu_{1m}\\ \nu_{2m}\end{bmatrix}.$$

Following the same steps as equations 2.8 to 2.9, this definition is equivalent to redefining the flavour Hamiltonian in matter as

$$\hat{H}_{\text{flavour}} = \frac{\Delta m_m^2}{4E}\begin{bmatrix}-\cos 2\theta_m & \sin 2\theta_m\\ \sin 2\theta_m & \cos 2\theta_m\end{bmatrix}. \tag{2.14}$$

Equating equations 2.14 and 2.11, we finally get the relationship between our old and new mixing angles:

$$\begin{aligned}\frac{\Delta m^2}{4E}\begin{bmatrix}-\cos 2\theta & \sin 2\theta\\ \sin 2\theta & \cos 2\theta\end{bmatrix} &\overset{!}{=} \frac{\Delta m_m^2}{4E}\begin{bmatrix}-\cos 2\theta_m & \sin 2\theta_m\\ \sin 2\theta_m & \cos 2\theta_m\end{bmatrix}\\ \implies \sin 2\theta_m &= \sin 2\theta\frac{\Delta m^2}{\Delta m_m^2}\\ &= \frac{\sin 2\theta}{\sqrt{(\cos 2\theta - A)^2 + \sin^2 2\theta}}\end{aligned} \tag{2.15}$$

Because we diagonalized the Hamiltonian in the mass basis and wrote the flavour Hamiltonian in this form, equation 2.6 is automatically valid and our oscillation probability is

$$P^m_{\nu_e\to\nu_\mu}(L,E) = \sin^2(2\theta_m)\sin^2\left(\frac{\Delta m_m^2 L}{4E}\right), \tag{2.16}$$

where the parameters in matter are given by equations 2.13 and 2.15.

This derivation shows that matter effects can be taken into account by a simple redefinition of the oscillation parameters, at least in the case of two neutrino flavours. For three neutrinos, the algebra is a lot more involved, and beyond the scope of this report. Ohlsson and Snellman[20] have shown that the same idea applies for three neutrino flavours, namely that we can express all oscillation parameters in matter by diagonalizing the matter Hamiltonian, and obtain the probability through the same formula

$$P^m_{\alpha\to\beta}(L,E) = \sum_i\sum_j U^m_{\alpha i}U^{m*}_{\beta i}U^{m*}_{\alpha j}U^m_{\beta j}\exp\left(-\mathrm{i}\frac{\Delta\tilde{m}^2_{ij}L}{2E}\right), \tag{2.17}$$

where U^m and $\Delta\tilde{m}^2_{ij}$ can be expressed in terms of U, Δm_{ij} and the eigenvalues and components of the Hamiltonian in matter. Although they only considered the case where

$\delta_{CP} = 0$, expressions for the parameters were later derived[21] in the general case, for any δ_{CP}.

Experiments in which neutrinos spend a significant amount of time propagating through matter — e.g. neutrinos from the sun's core, or neutrinos propagating underground through the Earth — require us to take matter effects into account in order to produce a realistic model. The DUNE experiment will be performed entirely underground with a baseline of 1300km, enough to have a significant effect on the oscillation probability from muon neutrinos to electron neutrinos, as we will demonstrate in the next chapter.

2.2.5 The state of neutrino oscillations

Neutrino oscillations are still far from being fully understood. Aside from the fact that they are not compatible with the Standard Model, the phenomenology of oscillations is not yet complete. While three of the parameters are now known with uncertainties of a few percent, the remaining three are expected to be fully constrained only by the current and next generation of experiments.

Known parameters

The solar mixing angle θ_{12} and the solar mass squared difference Δm^2_{21} were the very first parameters to be probed, since already in 1968 Davis et al.[22] reported a discrepancy between the expected and observed neutrino fluxes from the sun. In 2001, the SNO collaboration[23] reported direct evidence that the solar neutrino flux consisted only partly of electron-neutrinos by comparing their results to those of Super-K[24]. The solar neutrino problem was solved in 2002 by the KamLAND experiment[25]. By observing the disappearance of $\overline{\nu}_e$ produced in several nuclear reactors, they were able to exclude all solutions to the solar neutrino problem except for the "Large Mixing Angle" solution, whereby the solar parameters were estimated to be $\Delta m^2_{21} \approx 7.5 \times 10^{-5}$ eV^2 and $\theta_{12} \approx 0.59$.

In 1998, the Super-K collaboration[14] provided the first overwhelming evidence for the flavour oscillations of neutrinos through the observation of ν_μ disappearance in the flux of neutrinos produced by cosmic rays in the atmosphere. The results were consistent with values for the atmospheric parameters of $|\Delta m^2_{32}| \approx 10^{-3}$ eV^2 and $\sin^2 2\theta_{23} > 0.82$. These results were later improved upon by the MINOS[26], NOvA[27] and T2K[28] accelerator-based experiments.

Parameter	Value
Δm^2_{21}	$7.37 \times 10^{-5}\,\text{eV}^{-2}$
$\lvert\Delta m^2_{32}\rvert$	$2.56 \times 10^{-3}\,\text{eV}^{-2}$
θ_{12}	0.576
θ_{23}	0.710
θ_{13}	0.147

Table 2.1: Best-fit oscillation parameters from a global fit of past experiments.

The third mixing angle, θ_{13}, couples atmospheric and solar mixings in the PMNS matrix (see eq. 2.7). In addition, it is evident in the PMNS parametrization that a value of $\theta_{13} = 0$ would make the observation of CP violation in the lepton sector impossible. Hence this parameter plays a central role in the phenomenology of neutrino oscillations. Determining whether or not it is zero was one of the challenges of the past decade for neutrino physics. In 2011, T2K[29] rejected $\theta_{13} = 0$ with a 2.5σ significance. In 2012, the Daya Bay[30], RENO[31] and Double Chooz[32] reactor experiments reported their first results from $\overline{\nu}_e$ disappearance measurements: they established a small but non-zero θ_{13} with $\sin^2 2\theta_{13} \approx 0.1$, thus confirming the possibility of observing CP violation in subsequent neutrino oscillation experiments.

Table 2.1 lists the current best-fit values for the oscillation parameters, obtained from global fits of past experiments, and reported by the Particle Data Group[33].

Unknown parameters

While the absolute value of Δm^2_{32} is known with high precision, previous experiments have not been sensitive to its sign. The problem of whether the third mass eigenstate is heavier

or lighter than the other two is called the neutrino mass hierarchy — or mass ordering — problem. It is likely to be resolved by the next generation of long baseline neutrino experiments, as we will show in our results. Throughout this report, we will denote by "normal hierarchy" (NH) the case where the third mass eigenstate is heavier than the other two ($m_3^2 > m_2^2 > m_1^2$, and Δm_{32}^2 is a positive value), and by "inverted hierarchy" (IH) the case where it is lighter ($m_2^2 > m_1^2 > m_3^2$, Δm_{32}^2 negative).

The second unknown is the octant of θ_{23}. This parameter is known to lie around 45°, in either the first or second octant of the unit circle. However, experiments in the past have typically only been sensitive to $\sin^2 2\theta_{23}$, resulting in two possible degenerate values for θ_{23} that could fit the same data[5]. In order to break this degeneracy, a possible solution in accelerator-based experiments is to reverse the polarity of the pion-focusing field, hence making the beam contain anti-neutrinos rather than neutrinos. Counting ν_e appearance events under both polarities breaks the $\sin^2 2\theta_{23}$ degeneracy[34], enabling the measurement of the octant of θ_{23}.

The last unknown is the CP violating phase δ_{CP}. Unlike the other parameters, there are so far few constraints on its value. Because of its relationship to CP violation in the lepton sector, this parameter has a cosmological relevance since it could explain in part the overwhelming presence of matter over antimatter in the universe. Similarly to the other two parameters, it is expected that the next generation of neutrino experiments will determine δ_{CP}.

Although we use the standard three-neutrino framework throughout this report, it is relevant to mention that it may not be entirely accurate. The existence of sterile neutrinos — neutrinos which do not interact via the weak interaction, but do mix with the others via oscillations — has not been ruled out by oscillation experiments. The evidence for the existence of such particles would be the non-unitarity of the three-neutrino mixing matrix. Since δ_{CP} is still not fully constrained, it is so far impossible to rule out sterile neutrinos.

[5]Since $\sin(2(\pi/4 + x)) = \sin(2(\pi/4 - x))$ for any x.

Chapter 3

Methods

In this chapter, we will discuss the statistics of experimental sensitivity, our implementation of neutrino oscillations and how it fits into models of long-baseline neutrino experiments. We will concisely present examples of oscillation probability plots produced by our oscillation model, followed by a detailed section on the modelling of the DUNE experiment. At the end of the chapter, we will show our predictions for the sensitivity of both DUNE and Hyper-K to the mass hierarchy and to CP violation.

3.1 Statistical analysis

In this section, we will introduce qualitatively and quantitatively the definition of *sensitivity* in the context of neutrino oscillation experiments. With a short derivation, we will show that in the case of the mass hierarchy question, the $\Delta\chi^2$ statistic is Gaussian-distributed around its mean, $\overline{\Delta\chi^2}$, which is the quantity we will determine from our model and use as a measure of sensitivity.

3.1.1 Experimental sensitivity

Neutrino experiments are characterised by the extremely small scattering cross section of weak processes. Neutrinos are almost massless, have no charge, and being leptons, they are not affected by strong interactions. These unique properties make their detection particularly difficult and the associated experiments particularly costly and time-inefficient. The best way for experimentalists to compensate for a small cross section is to increase the scale of their detector.

The Sudbury Neutrino Observatory (SNO) experiment, which confirmed the existence of matter effects on neutrino oscillations in 2001, consisted of 1000 tons of heavy water enclosed in a sphere of diameter 12 meters[35]. The DUNE experiment, expected to start collecting data in 2024, will use 4850L of liquid argon for a total fiducial mass[1] of 40 kilotons[1]. For projects of this scale, it is crucial to try to maximize the time and cost efficiency of the experiment by optimizing its design. It is thus conventional as part of the design process to evaluate the experiment's sensitivity to the relevant physical parameters. This evaluation can be done concurrently with the evolution and refinement of the project. It can then be used to legitimize the project to the scientific community and attract the support of funding agencies.

In general, it may be ambiguous which design choices will lead to a better sensitivity. As a consequence, experimentalists have devised statistical methods to allow the quantifi-

[1] The outermost parts of the detector are more sensitive to background events. To account for this, all events outside the more reliable central region are discarded. The part of the total detector mass that remains is called fiducial mass.

cation of sensitivity in order to compare different designs or even different experiments, and to be able to do so in a mathematically rigorous way that is accepted by the most scientists. When applied, these methods also enable us to compare potential experiments that could have different characteristics — baseline, detector technology, neutrino source — and to understand the complementarities that could result from combining their results.

3.1.2 Sensitivity to the mass hierarchy

In a general experiment where a set of data y_i is collected, one can evaluate the goodness of fit between the data and a model using the χ^2 statistic:

$$\chi^2(\theta) = \sum_i \frac{(y_i - n_i(\theta))^2}{\sigma_i^2}, \tag{3.1}$$

where $n_i(\theta)$ are the values predicted by the model using a set of parameters θ, and σ_i is the uncertainty associated with the measurement y_i. This statistic can be minimized in parameter-space to yield the best-fit θ, i.e. the set of parameters that seems to most accurately describe Nature:

$$\chi^2_{\text{min}} = \min_\theta \sum_i \frac{(y_i - n_i(\theta))^2}{\sigma_i^2}. \tag{3.2}$$

If n measurements were made and θ contains p parameters, this minimum χ^2 will be distributed according to a χ^2 distribution with $n - p$ degrees of freedom, allowing us to determine a confidence level for rejecting the null hypothesis.

When trying to determine the mass hierarchy from data, one might want to use a test statistic which is more appropriate to this specific purpose. In order to more easily discriminate between the two possible hypotheses, namely NH and IH, we define

$$\Delta\chi^2 = \min_{\theta\in\text{IH}} \chi^2(\theta) - \min_{\theta\in\text{NH}} \chi^2(\theta), \tag{3.3}$$

where θ are oscillation parameters constrained to a particular mass hierarchy in the minimization. The sign of this statistic indicates which hierarchy seems to best fit our data. Its distribution, which in general is not a χ^2 distribution, gives us the confidence level at which we can reject one of the hierarchies.

In the context of future experiments, we cannot evaluate χ^2 since no measurements have been made. A standard procedure[36] to evaluate sensitivity is to replace the measurements y_i by the best prediction we can make with our model. Assuming that the true hierarchy is NH, and that the true parameters are θ_0, our "most probable data set[2]" is $n_i^{\text{N}}(\theta_0)$, where the superscript denotes the assumed true hierarchy. Substituting this for y_i in eqs. 3.2 and 3.3:

$$\overline{\Delta\chi^2}(\theta_0) = \min_{\theta\in\text{IH}} \sum_i \frac{(n_i^{\text{N}}(\theta_0) - n_i(\theta))^2}{\sigma_i^2} - \min_{\theta\in\text{NH}} \sum_i \frac{(n_i^{\text{N}}(\theta_0) - n_i(\theta))^2}{\sigma_i^2},$$

where the bar over $\Delta\chi^2$ indicates that it is associated with the most probable data set. Clearly, the second term vanishes since it is minimized over parameters that are compatible with the most probable data. We are left with

$$\overline{\Delta\chi^2}(\theta_0) = \min_{\theta\in\text{IH}} \sum_i \frac{(n_i^{\text{N}}(\theta_0) - n_i(\theta))^2}{\sigma_i^2}. \tag{3.4}$$

[2]Also referred to as Asimov data set.

Note that this is not a proper test statistic, since it does not depend on any measured data, but only on predictions. Heuristically, it is a measure of how incompatible the two hierarchies are in terms of the number of events we expect to measure in the experiment. Hence it makes sense to define eq. 3.4 as the sensitivity to the mass hierarchy[3]. However, we can be more quantitative in our treatment by determining the distribution of $\Delta\chi^2$ from eq. 3.3 and its relation to eq. 3.4. This will allow us to give a more rigorous statistical interpretation to the sensitivity.

Distribution of $\Delta\chi^2$ for the mass hierarchy

The mass hierarchy can only turn out to be normal (NH), or inverted (IH). As such, it is considered as a discrete, non-nested hypothesis — in contrast with a continuous variable such as δ_{CP} or θ_{23}. For this derivation, we consider the simple case where there are no nuisance parameters, as discussed in [37, 38]. Hence the set of parameters θ of eq. 3.1 is reduced to the choice of mass hierarchy, and the minimization of equation 3.3 is trivial.

We denote by y_i the event count recorded by a neutrino experiment per energy bin, where $i = 1, 2, ..., N$ is the index of the energy bin. Given that enough data has been collected, the event counts y_i will be distributed around their true value according to a Gaussian with variance $\sigma_i^2 = y_i$ (Poisson variable). Our model will yield predicted event counts that will depend on the true mass hierarchy. We denote by n_i^{N} the predicted count under normal hierarchy and by n_i^{I} the predicted count under inverted hierarchy. Let us assume that the true hierarchy — the one picked by Nature — is normally ordered. Then, assuming our model accurately describes Nature, we can write our experimental event counts as $y_i = n_i^{\mathrm{N}} + \sigma_i g_i$, where g_i is a random variable from a Gaussian distribution centered at zero and with variance 1. The $\Delta\chi^2$ statistic of equation 3.3 can then be written as

$$\begin{aligned}
\Delta\chi^2 &= \chi^2_{\mathrm{I}} - \chi^2_{\mathrm{N}} \\
&= \sum_i \frac{(y_i - n_i^{\mathrm{I}})^2}{\sigma_i^2} - \sum_i \frac{(y_i - n_i^{\mathrm{N}})^2}{\sigma_i^2} \\
&= \sum_i \frac{(n_i^{\mathrm{N}} + \sigma_i g_i - n_i^{\mathrm{I}})^2 - (n_i^{\mathrm{N}} + \sigma_i g_i - n_i^{\mathrm{N}})^2}{\sigma_i^2} \\
&= \sum_i \frac{(n_i^{\mathrm{N}} - n_i^{\mathrm{I}})^2}{n_i^{\mathrm{N}}} + \sum_i \frac{2(n_i^{\mathrm{N}} - n_i^{\mathrm{I}})}{n_i^{\mathrm{N}}} g_i,
\end{aligned} \tag{3.5}$$

where in the last step we have used the fact that $\sigma_i = \sqrt{y_i} \approx \sqrt{n_i^{\mathrm{N}}}$ when our event count is large. In this form, we can see that $\Delta\chi^2$ is a Gaussian-distributed variable where the mean is the first term of eq. 3.5:

$$\overline{\Delta\chi^2} \equiv \sum_i \frac{(n_i^{\mathrm{N}} - n_i^{\mathrm{I}})^2}{n_i^{\mathrm{N}}}, \tag{3.6}$$

and the standard deviation is

$$\sigma_{\Delta\chi^2} \equiv \sqrt{\sum_i \frac{4(n_i^{\mathrm{N}} - n_i^{\mathrm{I}})^2}{n_i^{\mathrm{N}}}} = 2\sqrt{\overline{\Delta\chi^2}}.$$

[3] If instead we assume the true hierarchy to be IH, our most probable data set is $n_i^{\mathrm{I}}(\theta_0)$ and we are left with only the second term:

$$\overline{\Delta\chi^2}(\theta_0) = -\min_{\theta \in \mathrm{NH}} \sum_i \frac{(n_i^{\mathrm{I}}(\theta_0) - n_i(\theta))^2}{\sigma_i^2}.$$

Hence, the sensitivity we evaluate from our model is actually the mean value of the $\Delta\chi^2$ statistic, whose purpose is to distinguish between the two hierarchies. Quantitatively, as shown by Blennow et al.[36], the square root of $\overline{\Delta\chi^2}$ in fact corresponds to the confidence level at which the experiment will be able to reject the inverted hierarchy with a 50% chance of type II error, i.e. a 50% chance to accept NH as the true hierarchy although it is not.

We recognize in eq. 3.6 the sensitivity of eq. 3.4 without the parameters θ. However, for neutrino oscillations, we cannot treat all the other parameters as constant since δ_{CP} and θ_{23} are not yet fully determined. In general, it will be more informative to use eq. 3.4 as a measure of sensitivity rather than eq. 3.6, although we lose the nice properties that we have outlined above, namely the $\Delta\chi^2$ statistic will no longer be exactly Gaussian-distributed. In this case, the distribution of $\Delta\chi^2$ must in general be determined explicitely through Monte Carlo simulations, which is beyond the scope of this report. It is however discussed and performed in [36] for the NOvA and DUNE experiments among others. Their results indicate that the $\Delta\chi^2$ statistic we define in eq. 3.3 is approximately Gaussian-distributed, at least in the context of DUNE. Thus, we may also apply the interpretation given in the previous paragraph to the more general sensitivity of eq. 3.4.

For simplicity, we will regard θ_{23} as a fixed parameter — not to be minimized — since its precise value does not affect the oscillation probability we calculate to model DUNE[4]. Hence, we can write the sensitivity to the mass hierarchy as

$$\overline{\Delta\chi^2}(\delta_0) = \min_{\delta} \sum_i \frac{(n_i^{\mathrm{N}}(\delta_0) - n_i^{\mathrm{I}}(\delta))}{n_i^{\mathrm{N}}(\delta_0)}, \tag{3.7}$$

where now we are only minimizing over $\delta_{CP} \in [-\pi, \pi]$, and δ_0 is our assumed true δ_{CP}. We will plot equation 3.7 as a function of δ_0 for the DUNE experiment later in this chapter, after discussing the DUNE model.

3.1.3 Sensitivity to CP violation

In addition to the sensitivity to the mass hierarchy, we can estimate the sensitivity to CP violation as a function of δ_{CP} using a similar statistic as eq. 3.7. The sensitivity to CP violation is the ability of the experiment to discriminate between values of δ_{CP} that violate CP and values that do not. The only values that do not violate CP are $\delta_{CP} = 0$ and $\delta_{CP} = \pi$. Hence we define

$$\overline{\Delta\chi^2}_{CPV}(\delta_0) \equiv \min\left(\sum_i \frac{(n_i(\delta_0) - n_i(0))^2}{n_i(\delta_0)}, \ \sum_i \frac{(n_i(\delta_0) - n_i(\pi))^2}{n_i(\delta_0)} \right), \tag{3.8}$$

where δ_0 is our assumed true value of δ_{CP}, and the assumed mass hierarchy is not specified for generality. In equation 3.8, we are evaluating a goodness of fit between a model where CP is violated and a model where CP is conserved (except for $\delta_0 = 0,\ \pi$; then $\overline{\Delta\chi^2}_{CPV} = 0$). This tells us, for every possible true value of $\delta_{CP} = \delta_0$, how badly the most probable data fits CP-conserving models; hence how easily CP conservation can be ruled out. We will also show plots of CP violation sensitivity at the end of this chapter.

In the case of the sensitivity to CP violation, the $\overline{\Delta\chi^2}$ we have defined in 3.8 does not, in general, correspond to the mean value of a $\Delta\chi^2$ statistic. In order to make such a claim, one would have to determine the distribution of $\Delta\chi^2$ through Monte Carlo techniques. Surprisingly, to the extent of our research, and unlike the case of the mass hierarchy sensitivity, this has not been done in the literature. It is thus impossible to assign to this $\overline{\Delta\chi^2}$

[4]More accurately, the octant of θ_{23} can only be measured if the LBNF is run in both neutrino and anti-neutrino mode[34]. In our model, we are only considering the neutrino mode, hence θ_{23} is effectively a fixed parameter.

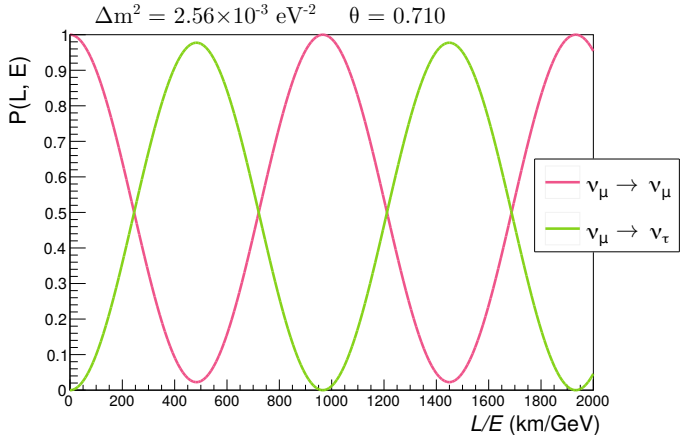

Figure 3.1: Oscillation probability vs. L/E for two neutrino flavours. The amplitude is governed by θ while the frequency is proportional to Δm^2. The mixing between flavours is almost maximal, i.e. the appearance of ν_τ is almost 100% at the half period.

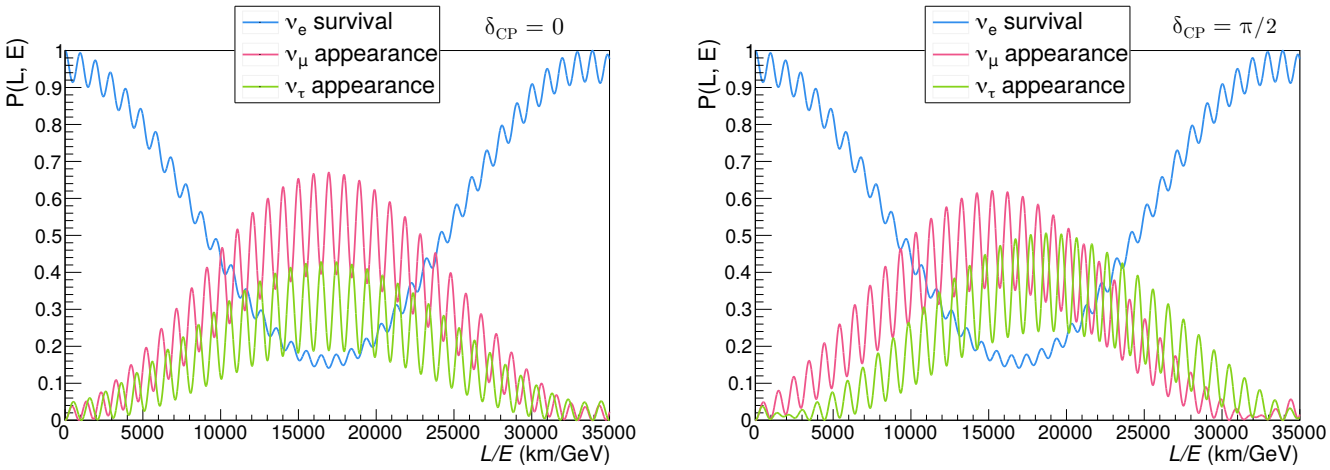

Figure 3.2: Oscillation probability for a neutrino produced as a ν_e, allowed to oscillate to ν_τ and ν_μ. The mass hierarchy is NH for both plots. We illustrate the difference made by the CP-violating phase by showing a plot where CP is conserved ($\delta_{CP} = 0$) and a plot where CP is maximally violated ($\delta_{CP} = \pi/2$).

a rigorous statistical interpretation, which is problematic. In retrospect, a solution would have been to perform the simulations ourselves and present the results here, although it would have required a significant time investment to refurbish the code for such a purpose.

3.2 Neutrino oscillation model

By implementing the concepts introduced in the previous chapter, we are able to model the oscillation of neutrinos through a vacuum or through matter.

The first step of our work was to implement in code the phenomenological oscillation formulae of chapter 2. The simplest test case is equation 2.6, the oscillation between two neutrino flavours. Figure 3.1 shows the oscillation probability of a neutrino initially produced as a ν_μ. For this plot, we picked the parameters Δm^2 and θ as the best-fit atmospheric parameters Δm^2_{32} and θ_{23} listed in table 2.1.

The next step is to implement three-neutrino oscillations. This involves implementing the complex PMNS matrix of eq. 2.7 and the more general probability function of eq. 2.4. Figure 3.2 shows the oscillation probability for a neutrino starting as a ν_e as a function of

L/E. In all the plots from figure 3.2 on, all oscillation parameters are the best-fit values listed in table 2.1 and the hierarchy and δ_{CP} are specified.

The difference between the two plots in figure 3.2 clearly shows that given all other parameters, it is possible to determine the true value of δ_{CP} by measuring neutrino appearance rates. Unfortunately, the problem is not that easily solved. In neutrino experiments, reconstructing the energy of neutrinos in the detector is difficult and prone to random and systematic errors. Additionally, while some parameters are known with good precision $(\theta_{12}, \theta_{13}, \Delta m^2_{21})$, the others remain elusive and challenging to measure independently of each other. Corrections must also be applied when the oscillations take place through matter. It is necessary to choose an appropriate and reliable model of the of the medium through which the neutrinos propagate, since the potential V_e of equation 2.10 is proportional to the electron density in the medium.

3.3 Model of an accelerator-based long baseline experiment

3.3.1 The DUNE experiment

The Deep Underground Neutrino Experiment[1] (DUNE) is a future long-baseline experiment designed — among other goals — to determine the CP violating phase δ_{CP}, the neutrino mass hierarchy (the sign of Δm^2_{31}) and the octant of θ_{23} (whether it is greater or less than $\pi/4$). It will make use of Fermilab's Long-Baseline Neutrino Facility (LBNF) in Batavia, Illinois for the production of a high-intensity neutrino beam aimed at the Sanford Underground Research Facility, 1300 km away, where the DUNE detectors will be built. Four liquid argon time-projection chambers (LArTPC) of fiducial mass 10 kt each will serve as detectors, with the ability to reconstruct the trajectories and kinematic quantities of interacting neutrinos.

DUNE will primarily observe the oscillations from ν_μ to ν_e in the LBNF beam. This appearance channel alone is expected to provide enough data to reach the objectives mentioned above, as we will show later. The neutrino beam will travel through the Earth's crust for 1300 km, hence matter effects must be taken into account. The DUNE experiment is thus a perfect candidate to try our simple model and see if we can reproduce results from the literature, namely predictions on the sensitivity of the experiment.

3.3.2 Event rate at the detector

In order to predict an event rate N in a general detector, we usually need three elements: the luminosity of the beam L, the interaction cross section σ, and the efficiency of the detector ϵ:

$$N = \epsilon L \sigma, \tag{3.9}$$

where L has units $\mathrm{m}^{-2}\mathrm{s}^{-1}$, σ has units m^2 and ϵ is unitless. We will use a modified version of this approach to predict event rates inside DUNE's liquid argon time-projection chamber (LArTPC), as a function of energy. While our model accurately describes the flavour oscillations of neutrinos, we are unable to estimate the neutrino flux coming out of the LBNF accelerator, or the efficiency of the LArTPC. For these two aspects we will rely on results presented by the DUNE collaboration in their conceptual design report (CDR).

To produce the neutrinos, the LBNF accelerates protons which collide with a graphite target to produce secondary mesons (π^+, π^-). These particles are focused along a decay pipe where they decay into muons and their associated muon neutrinos[39]. Hence by modelling the proton/target collision and the decay of secondary mesons, one can estimate the flux of neutrinos produced by the accelerator. The volume 3 of the CDR[40] provides the predicted flux of ν_μ and ν_e at the detector in the absence of oscillations. To

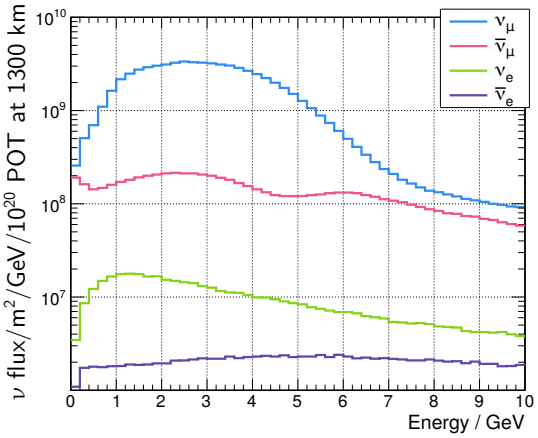

Figure 3.3: Predicted neutrino flux at the DUNE detector in the absence of oscillations, when focusing positively charged pions through the decay pipe. "POT" stands for protons on target. Reproduction of figure 6-2 from the DUNE CDR Vol. 3[40].

produce these results, they use the GEANT4[41] software to simulate the beamline from the reference design of the LBNF accelerator. Figure 3.3 shows a reproduction of the resulting plot from the DUNE CDR.

It is fairly simple to convert this "un-oscillated" spectrum into an "oscillated" one. Typically in accelerator-based experiments, the observed oscillation channel is the $\nu_\mu \to \nu_e$ appearance. Hence for each bin in the spectrum of figure 3.3, we multiply the un-oscillated muon-neutrino flux $\Phi_0^{(\mu)}$ (blue line) by the $\nu_\mu \to \nu_e$ oscillation probability:

$$\Phi_{\text{osc}}^{(e)}(E_i) = P_{\nu_\mu \to \nu_e}(E_i) \times \Phi_0^{(\mu)}(E_i), \tag{3.10}$$

where $\Phi_{\text{osc}}^{(e)}$ is the flux of electron-neutrinos resulting from ν_μ oscillations, and i indexes energy bins. We show this $P_{\nu_\mu \to \nu_e}$ function for different values of δ_{CP} and the two possible mass hierarchies on figure 3.4. We also illustrate the influence of matter effects on the appearance probability by showing oscillations in vacuum and in the Earth's mantle.

In general, the first (rightmost) peak[5] in the oscillation probability will provide the best signal, since it is wider than all other peaks on the energy axis, and thus easier to resolve. The first oscillation peak for the DUNE baseline $L = 1300\,\text{km}$ occurs between 1 and 10 GeV, and thus it is the energy range of choice for the DUNE experiment.

It is interesting to observe that matter effects enhance the amplitude of oscillations for the NH, and reduce it for the IH. The mass hierarchy only influences the sign of one of the mass-squared differences, thus in a vacuum it only affects the frequency of oscillations, as is shown on figures 3.4a and 3.4b: the peak amplitudes are left unchanged under a change of hierarchy. In vacuum, we can only change the amplitude by changing the mixing angles. We see in figures 3.4c and 3.4d that matter effects mix the parameters — as is manifest already for two neutrinos in equation 2.13 — in such a way that the mass hierarchy can impact the amplitude as well. This feature is crucial to DUNE's sensitivity to the mass hierarchy, as it will make discriminating between the two hypotheses much easier than if the neutrinos were propagating in empty space.

Now that we have the neutrino flux in the detector, i.e. the luminosity variable of equation 3.9, we would normally need a model of the weak interactions with the liquid argon (σ) and of the detector efficiency (ϵ). However another option is to normalize the

[5]It is the "first peak" because the probability falls to zero at higher energies. Note that the curves in figure 3.2 had L/E on the x-axis, while those in figure 3.4 are plotted against E. Hence the region covered by the latter corresponds to the "mirrored" leftmost part of the former.

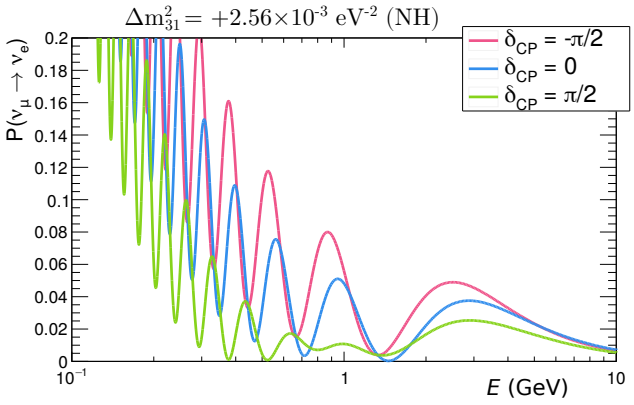

(a) Vacuum, NH

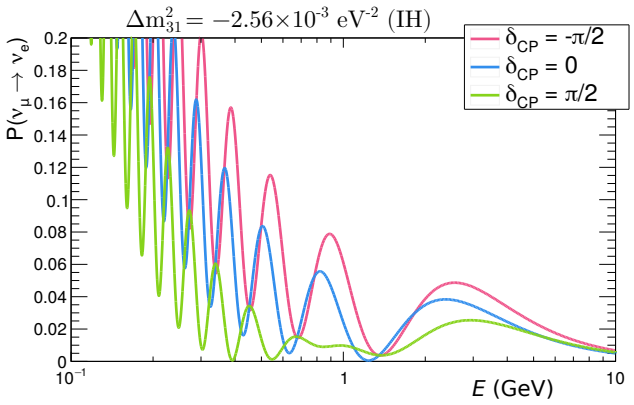

(b) Vacuum, IH

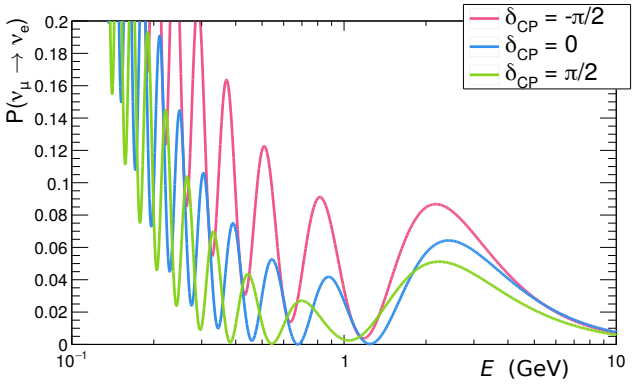

(c) Matter, NH

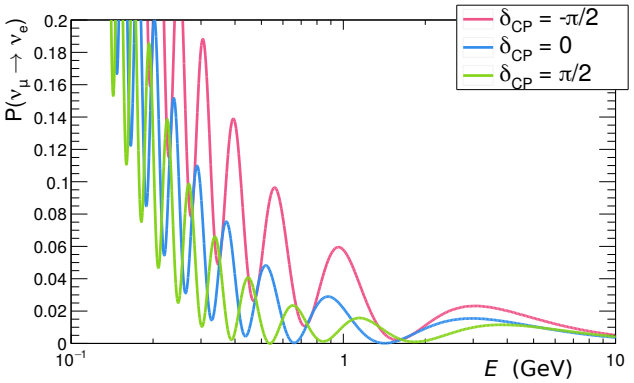

(d) Matter, IH

Figure 3.4: Oscillation probability $\nu_\mu \to \nu_e$ as a function of neutrino energy for neutrinos travelling over a baseline $L = 1300\,\text{km}$. Plots on the left have a normally ordered mass hierarchy, and plots on the right an inverted mass hierarchy. On top, neutrinos are oscillated in empty space, and on the bottom they are oscillated through matter of constant electron density $N_e = 2.2 N_A$ cm^{-3}, where N_A is Avogadro's constant[42]. All vacuum oscillation parameters are listed in table 2.1.

flux to the integrated event rate, i.e. the total number of events expected to be observed during a given exposure time. If we denote by N_{int} this integrated event rate, then the predicted event rate per unit energy is

$$\frac{\mathrm{d}N}{\mathrm{d}E} = \frac{N_{\text{int}}}{\int \Phi^{(e)}_{\text{osc}}(E)\ \mathrm{d}E} \times \Phi^{(e)}_{\text{osc}}(E). \tag{3.11}$$

In other words, we first normalize the flux spectrum $\Phi^{(e)}_{\text{osc}}$ to 1 by dividing it by its integral, and then normalize to the integrated event rate by multiplying by N_{int}. Since our flux is a function of discrete energy bins, we can rewrite this as

$$\begin{aligned} \frac{N_i}{\Delta E} &= \frac{N_{\text{int}}}{\sum_j \Phi^{(e)}_{\text{osc}}(E_j)\Delta E} \times \Phi^{(e)}_{\text{osc}}(E_i) \\ \implies N_i &= \frac{N_{\text{int}}}{\sum_j \Phi^{(e)}_{\text{osc}}(E_j)} \times \Phi^{(e)}_{\text{osc}}(E_i), \end{aligned} \tag{3.12}$$

where N_i is now the event rate per energy bin. Thus, from the integrated event rate, we are able to retrieve the event rate as a function of energy. We can then use this data to obtain the experiment's sensitivity to the mass hierarchy and δ_{CP}.

The CDR uses the GENIE[43] neutrino event generator and a parametrized detector response, to process the neutrino flux and obtain an event rate through Monte Carlo simulations. This complex modelling allows them to predict that the total number of CC events from ν_e appearance between 0.5 and 8 GeV during an exposure of 150 kt·MW·year will be $N^{\text{N}}_{\text{int}} = 861$ if the true hierarchy is normal, and $N^{\text{I}}_{\text{int}} = 495$ if it is inverted. Although both results assume that $\delta_{CP} = 0$, we will be able to calculate the event rates for all values of δ_{CP} using our model.

As can be seen in any of the graphs of figure 3.4, the area under the first appearance peak is different for different values of δ_{CP}. This indicates that the integrated event rate depends on δ_{CP}. The integrated event rate for any δ_{CP} is given by

$$\begin{aligned} N_{\text{int}}(\delta) &= \frac{\int P(\delta)\ \mathrm{d}E}{\int P(\delta = 0)\ \mathrm{d}E} \times N_{\text{int}} \\ &= \frac{\sum_j \Phi_j(\delta)}{\sum_j \Phi_j(\delta = 0)} \times N_{\text{int}}, \quad \text{using eq. 3.10}, \end{aligned} \tag{3.13}$$

where $P(\delta)$ is the $\nu_\mu \to \nu_e$ appearance probability for any $\delta_{CP} = \delta$, and $\Phi_j \equiv \Phi^{(e)}_{\text{osc}}(E_j)$. Thus, substituting into equation 3.12,

$$\begin{aligned} N_i(\delta) &= \frac{N_{\text{int}}(\delta)}{\sum_j \Phi_j(\delta)} \times \Phi_i(\delta) \\ &= \frac{N_{\text{int}}}{\sum_j \Phi_j(\delta)} \frac{\sum_j \Phi_j(\delta)}{\sum_j \Phi_j(\delta = 0)} \times \Phi_j(\delta) \\ &= \frac{N_{\text{int}}}{\sum_j \Phi_j(\delta = 0)} \times \Phi_j(\delta). \end{aligned} \tag{3.14}$$

Equation 3.14 allows us to calculate an event rate spectrum for any δ_{CP} using the integrated event rate from the CDR and two predicted fluxes we calculate using eq. 3.10. Figure 3.5 shows examples of such spectra, for two values of δ_{CP} and the two possible hierarchies.

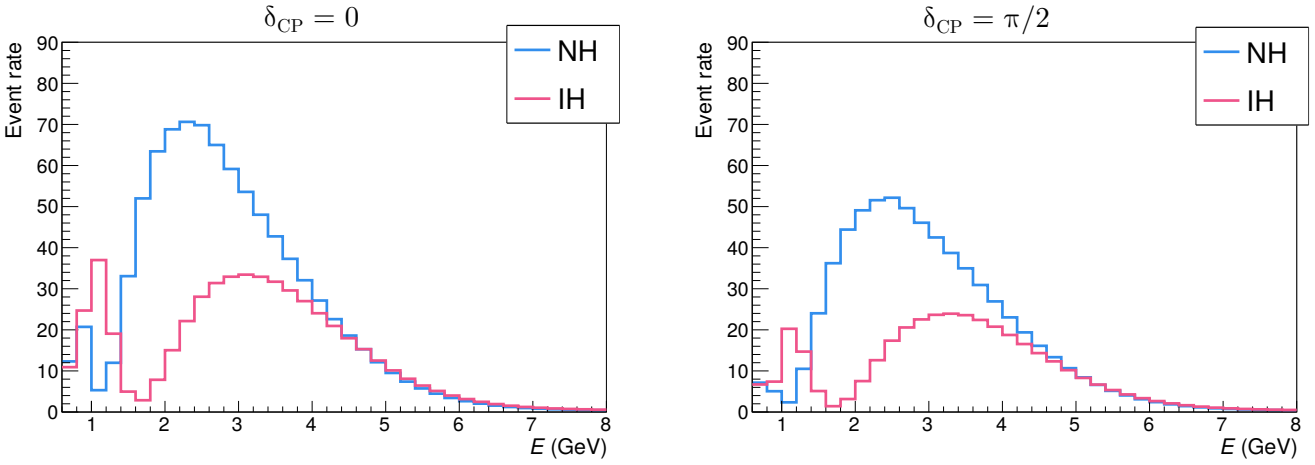

Figure 3.5: Predicted event rate spectra at DUNE as a function of neutrino energy, for two values of δ_{CP} and the two hierarchies. For $\delta_{CP} = 0$, the area under the curve (integrated event rate) is $N_{\text{int}}^{\text{N}} = 861$ for the blue line and $N_{\text{int}}^{\text{I}} = 495$ for the red line. For $\delta_{CP} = \pi/2$, the integrals are given by eq. 3.13.

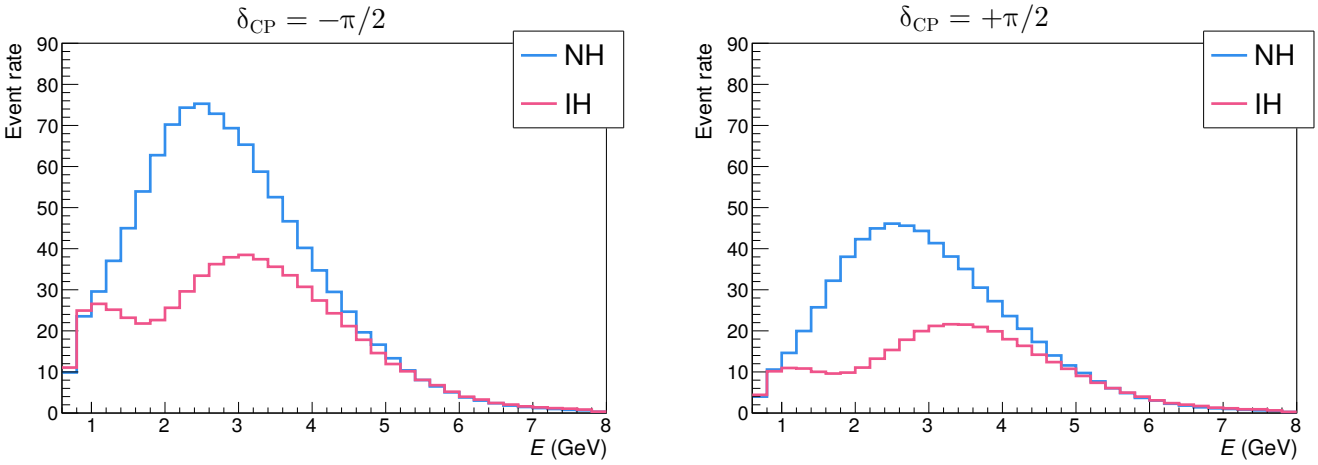

Figure 3.6: Predicted event rate spectra at DUNE after energy reconstruction. The statistical uncertainty on the energy of each event is picked to be $\sigma_E = 0.5\,\text{GeV}$.

3.3.3 Energy reconstruction

In order to produce a more realistic model, we can introduce by hand uncertainties on the energy reconstruction of neutrino events in the detector. The method is very straightforward: for each event in each energy bin i, we pick the reconstructed energy from a normal distribution around the true energy E_i. The event is then reassigned to the bin corresponding to the reconstructed energy.

Figure 3.6 shows examples of reconstructed event rate spectra for $\delta_{CP} = -\pi/2$ and $\delta_{CP} = \pi/2$. We observe that this simplistic energy reconstruction flattens out the event distribution, but also slightly shifts the oscillation maxima towards the high energies, hence introducing a systematic error in the event rate.

3.3.4 Sensitivity to the mass hierarchy and CP violation

With our event rate spectra under NH, IH, and any δ_{CP}, we can finally estimate the sensitivity of DUNE using the methods of section 3.1.

Figure 3.7 shows the mass hierarchy sensitivity of DUNE as defined in equation 3.7. It is useful now to recall the interpretation of sensitivity for the mass hierarchy, as shown

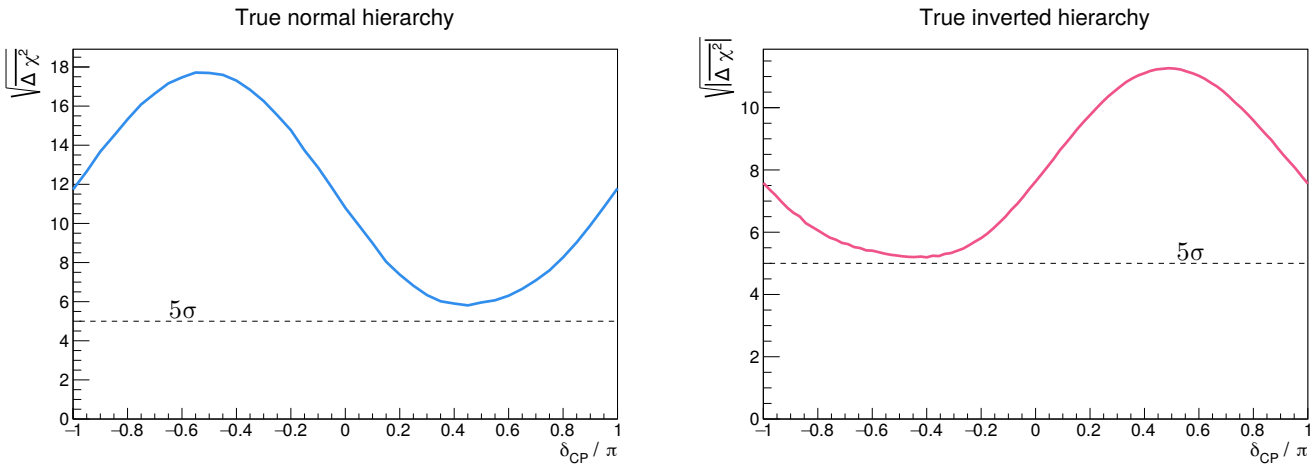

Figure 3.7: Sensitivity of DUNE to the neutrino mass hierarchy as a function of δ_{CP} and the true hierarchy, for an exposure of 150 kt·MW·year.

in [36]: the square root of $\overline{\Delta\chi^2}$ corresponds to the confidence level at which the experiment will be able to reject the false hierarchy with a 50% chance of type II error.

Qualitatively, we can see that if the mass hierarchy is normally ordered, DUNE will more efficiently reject IH if δ_{CP} lies around $-\pi/2$. On the other hand, if IH is the true hierarchy, a δ_{CP} around $\pi/2$ will be more favourable. Under an inverted hierarchy, the average sensitivity is lower than for NH, which can be explained by the overall smaller number of events expected to be observed under IH.

However, for both hierarchies, $\sqrt{|\overline{\Delta\chi^2}|}$ is greater than 5 for all values of δ_{CP}, hence we predict that *DUNE will reject the false hierarchy with a significance* $> 5\sigma$ *whatever the true combination of parameters turns out to be.* Comparing our results with the predictions published in the CDR, it is clear that we are slightly overestimating the sensitivity of DUNE to the mass hierarchy. In our model, we are only considering an exposure of 150 kt·MW·year in the "neutrino" mode of the LBNF accelerator, whereby positive pions are focused down the decay tunnel and the resulting flux is composed mostly of neutrinos. The DUNE experiment will also take data from the "anti-neutrino" mode, where the polarity of the focusing field is reversed in the LBNF accelerator. In the CDR, predicted sensitivities are given for an exposure of 150 kt·MW·year in neutrino mode plus 150 kt·MW·year in anti-neutrino mode, whereas we only consider the former. Despite this, our results and theirs are similar in terms of the significance in rejecting the false hierarchy, hence our previous conclusion that we are overestimating DUNE's sensitivity.

This discrepancy illustrates the fact that different methods were used to compute event rates, to simulate energy reconstruction, and possibly to estimate statistical uncertainties on the event rates. On this latter point, it can be noted that we have used throughout this work the approximation that event rates are Poisson variables with uncertainty given by their square root. In general, this is appropriate only when the event rates are large, which is not the case in all regions of the spectra (see figure 3.6). However, making such an approximation was necessary in order to keep the model as simple as possible, and the resulting predictions appear to be in the range of what is acceptable in this context.

Figure 3.8 shows the sensitivity of DUNE to CP violation, as defined in eq. 3.8. Unfortunately, since we did not go through the effort of determining the distribution of $\Delta\chi^2$ for CP violation, we are not in a position to make as strong a statement as we did for sensitivity to the mass hierarchy. However, we follow the conventions used in the literature and refer to $\sqrt{\overline{\Delta\chi^2}} = 3$ and $\sqrt{\overline{\Delta\chi^2}} = 5$ as the 3σ and 5σ significance on the discovery of CP violation, respectively (see for example [44, 45, 46, 47]).

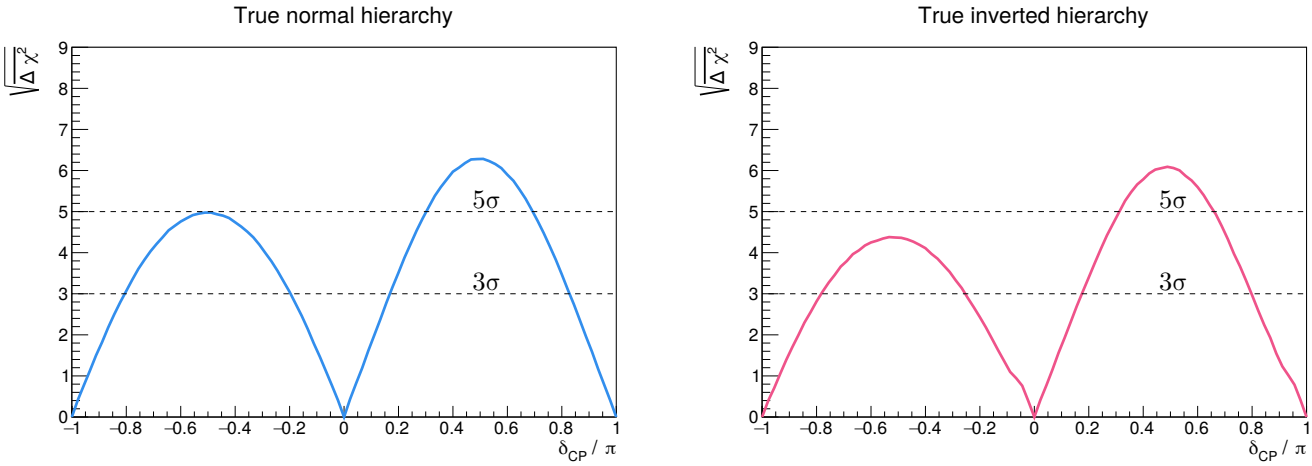

Figure 3.8: Sensitivity of DUNE to CP violation through neutrino oscillations, as a function of the true value of δ_{CP}, for an exposure of 150 kt·MW·year.

We predict a greater significance on CP violation discovery if δ_{CP} lies in the upper half circle $[0, \pi]$ for both mass hierarchies. The fraction of values of δ_{CP} for which the significance is greater than 5σ is relatively small, indicating that a longer exposure or complementary results from a different experiment are required to reduce the probability of error.

Again, our results are similar to those presented in the CDR, despite considering only the neutrino mode exposure. Hence it appears that our simple model is overestimating the sensitivity of DUNE to both the mass hierarchy and CP violation.

3.4 Hyper-K sensitivity

In order to have a point of reference to compare DUNE to, we applied the exact same procedure to a second future experiment. The Hyper-K detector is the planned upgrade to the SuperK detector in Japan. Fortunately for us, the Hyper-K design report[3] contains much the same information as the DUNE CDR, allowing us to reach the same results with minimal changes to the codebase.

While Hyper-K is also sensitive to atmospheric neutrinos, our model was originally designed for the purpose of modelling accelerator-based neutrinos only. Hence we consider only those neutrino events which arise from the J-PARC beam, without taking into account atmospheric events, or mis-identified beam events. The J-PARC accelerator is located 295 km away from the Hyper-K detector, which is a much shorter baseline than the LBNF-DUNE baseline of 1300 km.

In the design report, the performance of Hyper-K is estimated through models of the beamline and the Cherenkov detector. The expected number of ν_e appearance events after a 10-year runtime, assuming NH and $\delta_{CP} = 0$, is 2300. As discussed in section 3.3.2, this information is sufficient to extrapolate the expected number of events under both hierarchies and any δ_{CP}. Note that the sensitivity plots we present for DUNE and Hyper-K should be compared while keeping in mind that their respective exposures are not necessarily equivalent. While we quote an absolute exposure of ten years for Hyper-K, the quoted exposure 150 kt·MW·year for DUNE is relative to the final beam power and the detector's final fiducial mass.

We show the sensitivity of Hyper-K to the mass hierarchy and to CP violation in figures 3.9 and 3.10, respectively. Although the total number of events we record for Hyper-K is almost three times as many as for DUNE, the latter is overwhelmingly more

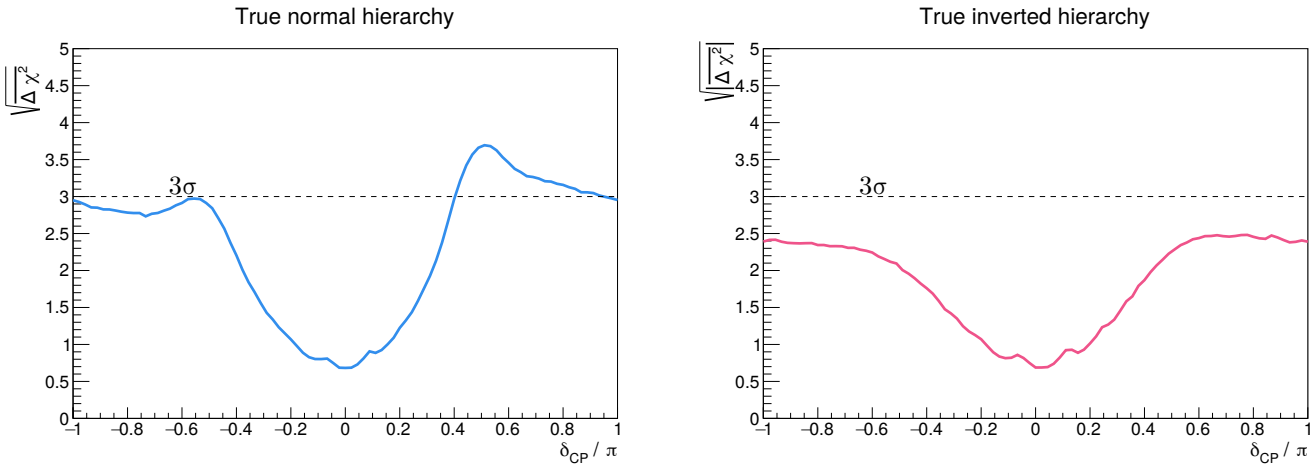

Figure 3.9: Sensitivity of Hyper-K to the mass hierarchy for an exposure to the J-PARC beam of 10 years, as a function of δ_{CP} and the mass hierarchy.

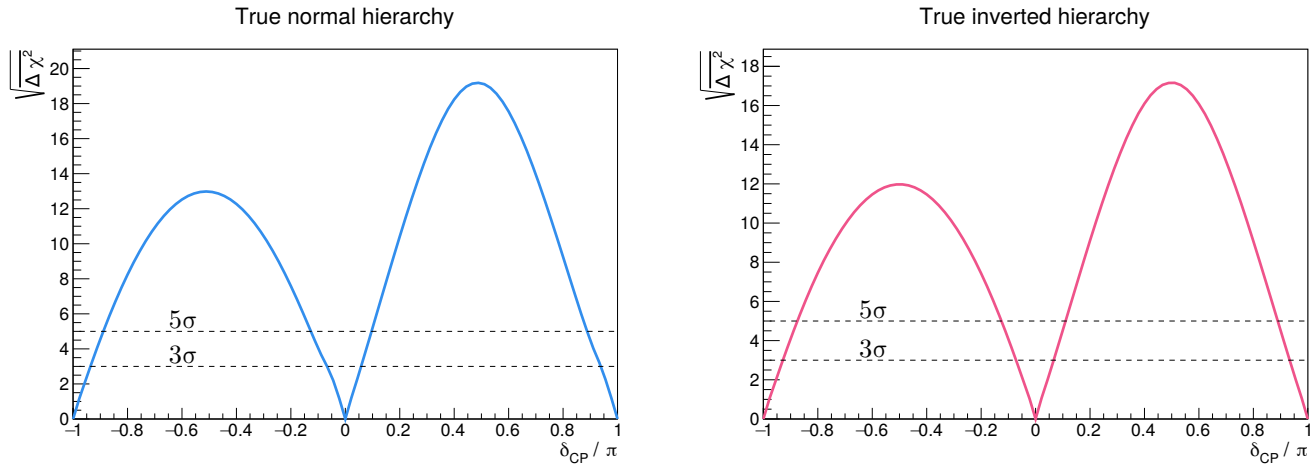

Figure 3.10: Sensitivity of Hyper-K to CP violation for an exposure to the J-PARC beam of 10 years, as a function of δ_{CP} and the mass hierarchy.

sensitive to the mass hierarchy. This is explained by the fact that at a baseline of 295 km, the effects of matter on the oscillations are small, and the dependence of the oscillation probability on the mass hierarchy is therefore weak.

The mass hierarchy determination significance, for Hyper-K, is smaller than 3σ for all values of δ_{CP} if IH is true. It is smaller than 5σ for all values of δ_{CP} if NH is true, and only greater than 3σ for about 30% of the possible δ_{CP} values. Keep in mind that since we are not taking into account the atmospheric neutrino events, we are only showing here a partial sensitivity. Furthermore, plans are being discussed[48] to build a second Hyper-K detector in the path of the J-PARC beam in Korea, at a baseline 1000-1300km. With a baseline similar to DUNE, this upgrade is expected to increase the mass hierarchy sensitivity of Hyper-K to a 6σ significance even for the least favourable δ_{CP} values.

On the other hand, in figure 3.10, we predict that *Hyper-K will be extremely sensitive to CP violation, ruling out CP conservation with a significance* $> 5\sigma$ *for 75% of possible values of* δ_{CP}. Comparing with the Hyper-K design report, our model seems to slightly overestimate the sensitivity, just as for DUNE. Hyper-K is more sensitive than DUNE to CP violation under their respective exposures, indicating a potential complementarity between the two future experiments.

In the next and final chapter, we will summarize and interpret our results and conclude by touching on the shortcomings of this project and the many ways in which it could be expanded through future work.

Chapter 4

Conclusion

4.1 Summary

It is clear that the next generation of experiments is being designed specifically to solve the remaining issues in the theory of neutrino oscillations. Using a simple model of neutrino oscillations and preliminary results from the designing groups, we are able to show quantitatively how sensitive we expect DUNE and Hyper-K to be to two of the as-yet-unknown oscillation parameters, namely the neutrino mass hierarchy and the CP-violating phase δ_{CP}.

From figure 3.7, we predict that DUNE, with an exposure of 150 kt·MW·year, will reject one of the hierarchies with a significance greater than 5σ under any combination of mass hierarchy and δ_{CP}. DUNE's sensitivity to CP violation (fig. 3.8) is fairly low, exceeding a 5σ significance for only about 10% of possible δ_{CP} values, for either hierarchy.

We predict that Hyper-K, after a 10-year exposure to the J-PARC beam, is much less sensitive to the mass hierarchy than DUNE despite recording more events. Its maximum mass hierarchy rejection significance is around 3σ (fig. 3.9). This poor sensitivity is due to the relatively short baseline (295 km). Because matter effects are weak at this baseline, the differences in the oscillation probability due to the mass hierarchy are small. The sensitivity of Hyper-K to CP violation (fig. 3.10) appears exceedingly high, being better than 5σ for 75% of the possible δ_{CP} values under either hierarchy. Such a high sensitivity can be seen as the result of suitable design choices for the beam and detector, which maximizes the expected event rate over the given exposure as well as the accuracy of the energy reconstruction process.

Evidently, the most beneficial outcome for neutrino physics would result from combining the two experiments, with DUNE rejecting one of the hierarchies and Hyper-K confirming or disproving CP violation. In reality, many more neutrino experiments are currently running and being designed, and the bigger picture is full of interesting details that are beyond the scope of this report, such as parameter degeneracies, the existence of sterile neutrinos or non-standard neutrino interations (see [34]).

Thus what we present here is merely a simplistic and incomplete picture, but it is hopefully a worthwhile attempt at providing insight into the future of neutrino oscillation experiments.

4.2 Shortcomings and future work

There are many ways in which this project is incomplete, some of which stand out more than others. One of them is that our model only considers the appearance events resulting from the neutrino mode of the respective accelerator. Both the LBNF and J-PARC beams are designed to be able to run in neutrino or anti-neutrino mode, i.e. it is possible to

reverse the focusing magnetic field such that anti-neutrinos are predominantly present in the beam. Both DUNE and Hyper-K are planned to collect data under both polarities. In addition to increasing the overall sensitivity (since more data is collected), this has the effect of breaking the θ_{23} octant degeneracy, as discussed in section 2.2.5.

Incidentally, there is also a parameter degeneracy in the combination of mass hierarchy and θ_{23} octant that cannot be resolved unless measurements in anti-neutrino mode are made as well[34]. If we denote by LO the case where θ_{23} lies in the lower octant and by HO the case where it lies in the higher octant, the degeneracy occurs between the combinations (NH, LO) and (IH, HO). That is, these two combinations of parameters result in the same oscillation probability. In theory, this would prevent DUNE from determining the true mass hierarchy if it only made measurements in neutrino mode, as long as the octant of θ_{23} was undetermined. To avoid this problem in our model, and for simplicity, θ_{23} was assumed to lie in the lower octant. A better model would consider both polarity modes and add the θ_{23} parameter to the analysis, resulting in an extra dimension in parameter space and a greater and more accurate insight into the potential outcomes of the experiment.

Secondly, as pointed out in section 3.1.3, we do not explicitely evaluate the distribution of the CP violation test statistic $\Delta\chi^2_{CPV}$, which impedes our ability to interpret CP violation sensitivity results. A more thorough study would include explicit determination of the distributions of both the mass hierarchy test statistic $\Delta\chi^2$ of equation 3.3 as well as $\Delta\chi^2_{CPV}$, through Monte Carlo simulations of the experiment.

Thirdly, our results are given only for a fixed value of the exposure of the detector to the beam. A straightforward extension to the code would allow us to determine the sensitivity *as a function of exposure*. From this information, a value of the "critical exposure" could be extracted. We could define this value, for example, as the exposure for which the mass hierarchy rejection significance is greater than 5σ for all values of δ_{CP}. Coincidentally, for DUNE, our results seem to indicate that this critical exposure is quite close to 150 kt·MW·year (see figure 3.7).

In section 3.4, we quickly mentioned the construction of a second Hyper-K detector in Korea. Again, with minor additions to the code, the increase in sensitivity of the Hyper-K experiment could have been evaluated, leading to more relevant results.

Finally, and although it would require significantly more work to make the code flexible enough, the model could be expanded to atmospheric neutrinos, in order to more realistically model Hyper-K, and to allow the incorporation of experiments such as IceCube collaboration's PINGU, ICAL, and others.

Acknowledgements

I am grateful to my supervisor, Dr. Lisa Falk, for being always insightful and supportive.
I also thank my family for their backing and my friends for their inexhaustible cynicism.

Bibliography

[1] DUNE Collaboration. Long-Baseline Neutrino Facility (LBNF) and Deep Underground Neutrino Experiment (DUNE) Conceptual Design Report Volume 2: The Physics Program for DUNE at LBNF. *Fermilab*. arXiv:1512.06148. 2015.

[2] The ROOT team. ROOT framework for data processing. https://root.cern.ch.

[3] Hyper-Kamiokande proto-collaboration. Hyper-Kamiokande Design Report. *KEK Preprint.* 2016.

[4] DUNE Collaboration. Long-Baseline Neutrino Facility (LBNF) and Deep Underground Neutrino Experiment (DUNE) Conceptual Design Report. *Fermilab*.

[5] Pauli W. Open letter to the group of radioactive people at the Gauverein meeting in Tübingen. 4 Dec 1930.

[6] Cowan C L Jr, Reines F, Harrison F B, Kruse H W, McGuire A D. Detection of the Free Neutrino: a Confirmation. *Science,* ***124****, 3212.* 1956.

[7] Zuber K. Neutrino Oscillations. *IOP Publishing*. 2004.

[8] Pontecorvo B. Electron and muon neutrinos. *Soviet Physics JETP,* **10, 1236**. 1960. Reprinted in Cambridge Monographs on Particle Physics, Nuclear Physics, and Cosmology, edited by Winter K. *Cambridge University Press*. 1991.

[9] Danby G, Gaillard J-M, Goulianos K, Lederman L M, Mistry N, Schwartz M, Steinberger J. Observation of High-Energy Neutrino Reactions and the Existence of Two Kinds of Neutrinos. *Phys. Rev. Letters,* **9, 1**. 1962.

[10] Pontecorvo B. Neutrino experiments and the problem of conservation of leptonic charge. *Soviet Physics JETP,* ***26****, 984.* 1968.

[11] DONUT Collaboration. Observation of Tau Neutrino Interactions. arXiv:hep-ex/0012035. 2000.

[12] Smirnov A Yu. Solar neutrinos: Oscillations or No-oscillations? arXiv:1609.02386. 2016.

[13] Schwichtenberg J. Physics From Symmetry (2nd Ed.). *Springer International Publishing.* 2018.

[14] The Super-Kamiokande Collaboration. Evidence for oscillation of atmospheric neutrinos. arXiv:hep-ex/9807003. 1998.

[15] Cohen A, Glashow S, Ligeti Z. Disentangling neutrino oscillations. *Physics Letters B,* ***678****, Issue 2.* 2008.

[16] Langacker P. The Standard Model and Beyond (2nd Ed.). *CRC Press*. 2017.

[17] Wolfenstein L. Neutrino oscillations in matter. *Phys. Rev. D* ***17****, 2369*. 1978.

[18] Mikheyev S, Smirnov A. Resonance enhancement of oscillations in matter and solar neutrino spectroscopy. *Soviet Journal of Nuclear Physics* ***42:6***. 1985.

[19] Ricciardi S. Lecture Notes on Neutrino oscillations in matter. http://hepwww.rl.ac.uk/ricciardi/Lectures/MSW-1.pdf. 2013.

[20] Ohlsson T, Snellman H. Three flavor neutrino oscillations in matter. arXiv:hep-ph/9910546. 1999.

[21] Kneller J, McLaughlin G. Three Flavor Neutrino Oscillations in Matter: Flavor Diagonal Potentials, the Adiabatic Basis and the CP phase. arXiv:0904.3823. 2009.

[22] Davis R Jr, Harmer D, Hoffman K. Search for Neutrinos from the Sun. *Phys. Rev. Lett.* ***20****, 1205*. 1968.

[23] SNO Collaboration. Measurement of the Rate of $\nu_e + d \rightarrow p + p + e^-$ Interactions Produced by ^8B Solar Neutrinos at the Sudbury Neutrino Observatory. *Phys. Rev. Lett.* ***87****, 071301*. 2001.

[24] Super-Kamiokande Collaboration. Solar ^8B and hep Neutrino Measurements from 1258 Days of Super-Kamiokande Data. *Phys. Rev. Lett.* ***86****, 5651*. 2001.

[25] KamLAND Collaboration. First Results from KamLAND: Evidence for Reactor Anti-Neutrino Disappearance. *Phys. Rev. Lett.* ***90****, 021802*. 2003.

[26] MINOS Collaboration. Combined Analysis of ν_μ Disappearance and $\nu_\mu \rightarrow \nu_e$ Appearance in MINOS Using Accelerator and Atmospheric Neutrinos. *Phys. Rev. Lett.* ***112****, 191801*. 2014.

[27] NOνA Collaboration. Measurement of the Neutrino Mixing Angle θ_{23} in NOνA. *Phys. Rev. Lett.* ***118****, 151802*. 2017.

[28] T2K Collaboration. Combined Analysis of Neutrino and Antineutrino Oscillations at T2K. *Phys. Rev. Lett.* ***118****, 151801*. 2017.

[29] T2K Collaboration. Indication of Electron Neutrino Appearance from an Accelerator-Produced Off-Axis Muon Neutrino Beam. *Phys. Rev. Lett.* ***107****, 041801*. 2011.

[30] Daya Bay Collaboration. Observation of Electron-Antineutrino Disappearance at Daya Bay. *Phys. Rev. Lett.* ***108****, 171803*. 2012.

[31] RENO Collaboration. Observation of Reactor Electron Antineutrinos Disappearance in the RENO Experiment. *Phys. Rev. Lett.* ***108****, 191802*. 2012.

[32] Double Chooz Collaboration. Indication of Reactor $\overline{\nu}_e$ Disappearance in the Double Chooz Experiment. *Phys. Rev. Lett.* ***108****, 131801*. 2012.

[33] Particle Data Group. Review of Neutrino Masses, Mixing and Oscillations. https://http://pdg.lbl.gov/2017/reviews/rpp2017-rev-neutrino-mixing.pdf. 2017.

[34] Raut S. Synergies and complementarities between proposed future neutrino projects. arXiv:1712.02096. 2017.

[35] Thomson M. Modern Particle Physics. *Cambridge University Press*. 2013.

[36] Blennow M, Coloma P, Huber P, Schwetz T. Quantifying the sensitivity of oscillation experiments to the neutrino mass hierarchy. arXiv:1311.1822. 2013.

[37] Ciuffoli E, Evslin J, Zhang X. Sensitivity to the Neutrino Mass Hierarchy. arXiv:1305.5150. 2013.

[38] Qian X, Tan A, Wang W, Ling JJ, McKeown RD, Zhang C. Statistical Evaluation of Experimental Determinations of Neutrino Mass Hierarchy. arXiv:1210.3651. 2012.

[39] Papadimitriou V, et al. Design of the LBNF beamline. arXiv:1704.04471. 2017.

[40] DUNE Collaboration. Long-Baseline Neutrino Facility (LBNF) and Deep Underground Neutrino Experiment (DUNE) Conceptual Design Report Volume 3: Long-Baseline Neutrino Facility for DUNE. *Fermilab*. 2015.

[41] The GEANT4 Collaboration. GEANT4 — a simulation toolkit. *Nuclear Instruments and Methods in Physics Research,* ***506****, Issue 3.* 2003.

[42] Freund M, Ohlsson T. Matter Enhanced Neutrino Oscillations with a Realistic Earth Density Profile. arXiv:hep-ph/9909501. 1999.

[43] Andreopoulos C, et al. The GENIE Neutrino Monte Carlo Generator. arXiv:0905.2517. 2009.

[44] Ballett P, King S, Pascoli S, Prouse N, Wang T. Sensitivities and synergies of DUNE and T2HK. arXiv:1612.07275. 2016.

[45] Martin-Albo J. Sensitivity of DUNE to long-baseline neutrino oscillation physics. arXiv:1710.08964. 2017.

[46] LAGUNA-LBNO Collaboration. The LBNO long-baseline oscillation sensitivities with two conventional neutrino beams at different baselines. arXiv:1412.0804. 2014.

[47] Masud M, Mehta P. Non-standard interactions spoiling the CP violation sensitivity at DUNE and other long baseline experiments. arXiv:1603.01380. 2016.

[48] Hyper-Kamiokande proto-collaboration. Physics Potentials with the Second Hyper-Kamiokande Detector in Korea. arXiv:1611.06118. 2016.